Impedance Spectroscopy, Strength and Limitations

Bernard A. Boukamp, University of Twente (The Netherlands)

Manuskripteingang: 7. Juli 2004; zur Veröffentlichung angenommen: 12. Juli 2004

Electrochemical impedance spectroscopy (EIS) has become an important tool in Solid State Electrochemistry. Simple Kramers-Kronig transform data validation assures selection of high quality data for subsequent CNLS-fit analysis. Optimized starting parameters and probable equivalent circuit can be obtained through a de-convolution based pre-analysis procedure. Combination of time-domain measurements with frequency-domain analysis extends impedance measurements in to the μHz range.

Keywords: Impedance spectroscopy, Kramers-Kronig transforms, data validation, deconvolution, time to frequency transform

Impedanzspektroskopie, Stärken und Grenzen

Die elektrochemische Impedanzspektroskopie (EIS) hat sich zu einem wichtigen Werkzeug der Festkörperelektrochemie entwickelt. Mittels einfacher Kramers-Kronig-Transformation werden die Daten validiert und selektiert und anschließend durch CNLS-Fits (Complex Nonlinear Least Squares) analysiert. Hierbei ist es wichtig, optimierte Startparameter und dem zu untersuchenden System angepasste Ersatzschaltbilder zu bestimmen. Dies geschieht durch eine Voranalyse, die auf einem Entfaltungsverfahren beruht. Die Kombination von Messung im Zeit-Raum und Datenanalyse im Frequenz-Raum erlaubt Impedanzmessungen bis in den μHz-Bereich.

Schlagwörter: Impedanzspektroskopie, Kramer-Kronig-Tranformation, Datenauswertung, Entfaltung, Zeit-Frequenz-Transformation

1 Introduction

The transport and transfer processes in electrochemical systems (solid or liquid) can be measured in the time domain, e. g. time dependence of the current response to a voltage step, or in the frequency domain where the impedance (complex resistance) or admittance (conductance) is obtained. The advantages of time domain measurements are:

- Simple and cheap instrumentation.
- Responses can be measured over large time periods (up to hours and more).
- Data acquisition is straightforward while digital noise filtering improves the long time data.

The main disadvantage is, however, the complicated data analysis, which often requires approximate solutions for the short and long time ranges.

The advantages of the frequency domain measurements are:

- More visual information on various contributing processes (different representations of data: impedance, admittance modulus, etc.).
- Generally an analytical expression is available for the impedance (transfer function), which can be

obtained from the solution in the Laplace domain of the time domain boundary problem definition.
- Large frequency domain available (from mHz to GHz and higher) with high accuracy.
- Powerful data analysis programs are available (Complex Nonlinear Least Squares fit or CNLS-fit). Error estimates for model parameters can be obtained.

The main disadvantage of the frequency domain measurements (Impedance Spectroscopy) is the costly instrumentation. Also obtaining good quality data at very low frequencies is not simple. But here both methods can be combined as will be presented below.

2 CNLS-fit Procedures

Most of the commercially available programs (e. g. LEVM by *J. Ross Macdonald* [1] or EquivCrt by *B.A. Boukamp* [2]) employ the Marquardt-Levenberg algorithm [3]. This algorithm combines a 'steepest descent' search, which is fast far from the minimum, with an 'analytical' search close to the minimum in the object function. The object function is defined as:

$$S = \sum_{i=1}^{N} w_i \left\{ \left[Z_{re,i} - Z_{re}(\omega_i, a_k) \right]^2 + \right. \\ \left. + \left[Z_{im,i} - Z_{im}(\omega_i, a_k) \right]^2 \right\} \quad (1)$$

where $Z_i = Z_{re,i} + jZ_{im,i}$ is the measured (complex) impedance and $Z(\omega_i, a_k) = Z_{re}(\omega_i, a_k) + jZ_{im}(\omega_i, a_k)$ is the model function with $a_k (k = 1 \ldots M)$ the adjustable parameters. w_i is the weight factor, which conveniently can be equated to the inverse of the square of the vector length of the impedance, $|Z(\omega_i)|$. The model function can often be presented by an 'equivalent circuit', built up from series and parallel connections of simple dispersive elements (e. g. resistance, capacitance, Warburg, etc.).

This generally non-linear model function is linearised through a Taylor series expansion, ignoring higher order terms. As a consequence, the procedure requires high quality starting values for the adjustable parameters, a_k. In Section 4 a method is illustrated to obtain good quality starting values as well as a plausible model function in terms of an equivalent circuit.

Scientists have been trying to avoid the starting values problem by employing different techniques. The Nelder-Meat (or Simplex) algorithm [4] does not require derivatives of the object function. Application is quite straightforward [5]. The method is very robust, i. e. little chance of a computer crash, but it is also slow. Secondly, there is always the possibility of converging into a secondary minimum. Hence frequent restarts are necessary. This secondary minimum problem can be avoided by using a 'Genetic Algorithm' [6], which continuously searches a predefined area in parameter space. This method has been tested successfully on reasonably simple systems. How well it performs on more complex 'real life data' has yet to be demonstrated.

All these methods share another problem: a model function must be available. In many instances the appropriate choice will be quite clear, but small contributions to the overall impedance of less obvious processes may not be noticed from visual inspection of the impedance or admittance graphs alone.

Yet, inspection of a simple representation of the CNLS-fit residuals, defined as:

$$\Delta_{re} = \frac{Z_{re,i} - Z_{re}(\omega_i, a_k)}{|Z(\omega_i, a_k)|}, \quad \Delta_{im} = \frac{Z_{im,i} - Z_{im}(\omega_i, a_k)}{|Z(\omega_i, a_k)|} \quad (2)$$

versus frequency will indicate whether the analysis was appropriate. For an optimum fit the residuals should scatter around the frequency axis, presenting the noise in the data.

3 Data validation

An impedance measurement is generally performed after changing an extensive parameter, e. g. temperature, partial pressure and/or polarisation. It will take time before the system has reached the new equilibrium state. In order to obtain reliable CNLS-analysis of the impedance data the system must be in equilibrium over the entire frequency range. Also aging and non-linear effects that can be due to non-linear electrode responses, can seriously affect the data analysis. The most effective way to test for possible non-equilibrium problems are the Kramers-Kronig transformations [7] that link an imaginary impedance value, $Z_{im}(\omega)$, to the complete set of real impedance values according to:

$$Z_{im}(\omega) = \frac{2\omega}{\pi} \int_0^\infty \frac{Z_{re}(x) - Z_{re}(\omega)}{x^2 - \omega^2} \, \mathrm{d}x \quad (3)$$

and the real value, $Z_{re}(.\omega)$, to the complete set of imaginary impedance values (apart from the high frequency cut-off value, R_∞):

$$Z_{re}(\omega) = R_\infty + \frac{2}{\pi} \int_0^\infty \frac{xZ_m(x) - \omega Z_{im}(\omega)}{x^2 - \omega^2} \, \mathrm{d}x \quad (4)$$

Eqs. (3) and (4) are only fulfilled when the conditions of *i*) causality, *ii*) linearity and *iii*) stability are met. The Kramers-Kronig conditions also call for *iv*) finiteness of the impedance over the entire frequency range, but for the data analysis this condition can be relaxed [7].

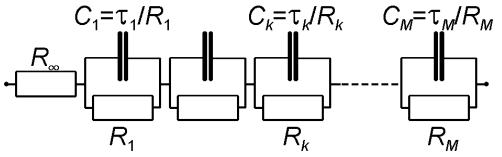

Figure 1: Arrangement of the series of (*RC*) circuits used in the Kramers-Kronig data validation test.
Bild 1: Anordnung der (*RC*)-Schaltkreise für die Validierung nach Kramers-Kronig.

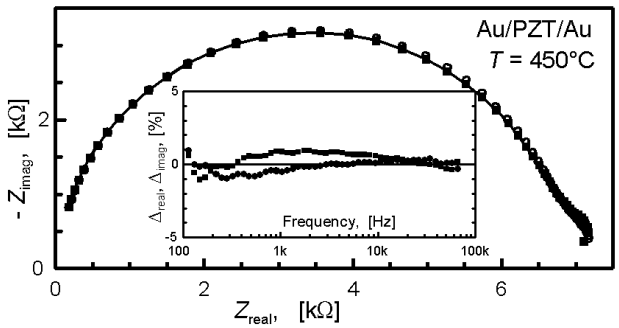

Figure 2: Impedance spectrum for a non-equilibrium measurement. Insert shows the traces of the residuals (comparison between data and KK-fit using eq. (5)).
Bild 2: Impedanzspektrum einer Nichtgleichgewichtsmessung. Eingefügt ist die Spur der Differenz zwischen Datensatz und KK-Fit bei Verwendung von Gl. (5).

A major problem, however, is the required integration from zero to infinity, which presents an experimental impossibility. Attempts have been made to use extrapolations, but then assumptions have to be made for a suitable model, which will have a strong influence on the quality of the transform test. Restricting the integrations to the frequency range employed seriously compromises the validation of measurements in the end ranges, which are especially those areas where non-KK behaviour might be suspected.

In a recent development only the measured frequency range is used. The data is fitted to a set of series connected (*RC*) circuits, Fig. 1. The reasoning is as follows: each parallel (*RC*) circuit is KK transformable; hence the entire circuit of connected (*RC*) circuits is KK transformable. When this circuit can be fitted to the data within acceptable limits, the data set must be KK transformable. Thus a KK validation can be performed without prior assumptions on specific models. In this process the time constants, τ_k, are predefined, with about 7 logarithmically spaced τ-values per decade in a time range that is the inverse of the applied frequency range. Hence the KK-validation function:

$$Z_{\mathrm{KK}}(\omega_i) = R_\infty + \sum_{k=1}^{M} \frac{R_k}{1+(\omega_i\tau_k)^2} - j\frac{R_k\omega_i\tau_k}{1+(\omega_i\tau_k)^2} \qquad (5)$$

must be fitted to the data set, which results in solving a set of M linear equations in R_k. A single matrix inversion is sufficient to obtain the R_k-vector [7]. The best way to compare the data set with the KK set is by plotting the residuals, eq. (2), versus frequency. A clear trace in the residuals plot will indicate non-KK behaviour. For well-behaved data scatter of the residuals around the frequency axis should be observed. Figure 2 shows the residuals plot for the KK transform test for impedance data of a lead-zirconate-titanate (PZT) sample, measured too quickly after a temperature change.

Comparing the residuals plot for the subsequent CNLS-fit with the KK data validation can then indicate whether the data is corrupted or that the model function is inappropriate, incomplete or 'too ideal', which can be the case for dimensionally distributed systems like porous gas electrodes for SOFC applications.

4 Pre-analysis by de-convolution

The overall impedance or admittance does not always show the number of time constants (transport, transfer and relaxation processes) that contribute to the frequency dispersion. Using just a simple equivalent circuit may yield visually an acceptable fit in the impedance or admittance representation, or even a seemingly excellent fit in a Bode representation. Proper analysis, however, can yield more information on the contributing processes. As an example we present the de-convolution analysis [8] of an impedance for a PZT sample measured at 400 °C in air [9], using dense gold electrodes. It is assumed that the material shows electronic conductivity and possibly also ionic conductivity. The impedance diagram is presented in Fig. 3.

From the low frequency intercept the electronic resistance is obtained, while the dielectric response can be extracted from the high frequency part in the admittance representation. The dielectric response has the form of a 'constant phase element' or CPE, which is defined in the admittance representation as: $Y_{\mathrm{CPE}} = Y_0(j\omega)^n$, with $n \leq 1$. Subtracting both elements as being in parallel with the ionic path a new dispersion is obtained, see Fig. 4.

The high frequency arc is now interpreted as grain boundary dispersion, while the low frequency part has

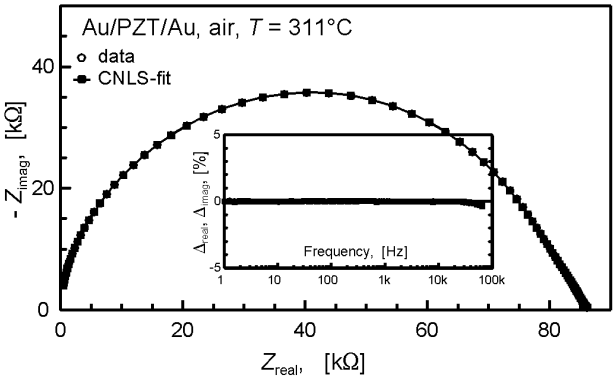

Figure 3: Impedance of a PZT sample with gold electrodes. Both data points and CNLS-fit are presented. The insert shows the distribution of the residuals.
Bild 3: Impedanz einer PZT-Probe mit Goldelektroden. Datensatz und CNLS-Fit sind dargestellt. Der Differenzplot ist eingefügt.

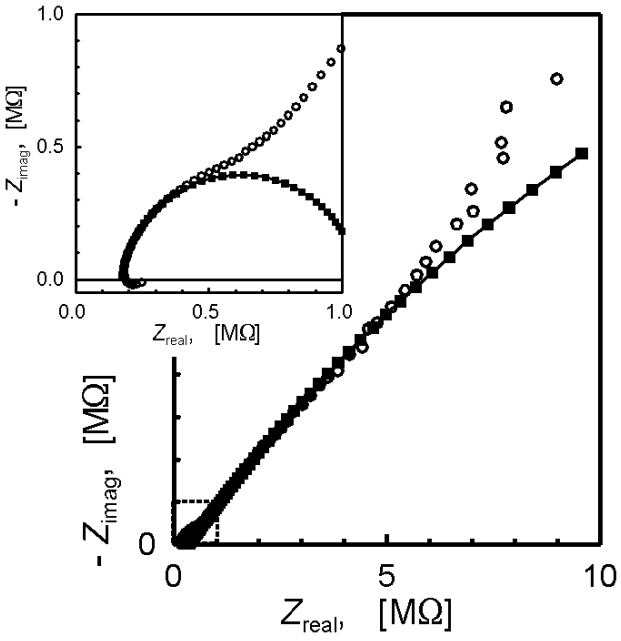

Figure 4: Impedance diagram after subtraction of the dielectric response and the electronic conductivity. Insert shows enlargement of the high frequency part. Solid squares present the partial $R(RQ)$ fits, see text.
Bild 4: Impedanzspektrum nach Subtraktion des dielektrischen Beitrages und der elektronischen Leitfähigkeit. Eine Vergrößerung des Hochfrequenzbereiches ist eingefügt. Die schwarzen Quadrate zeigen den partiellen $R(RQ)$-Fit, s. Text.

the character of a Randles type electrode dispersion. First the high frequency arc is approximated with a $R(RQ)$ circuit, see insert in Fig. 4. Next the part of the low frequency dispersion is also modelled with a second $R(RQ)$ circuit. As there is considerable overlap between the two semi-circles a third partial fit is performed with a $R(RQ)(RQ)$ circuit, using the previously obtained parameters as input. Such an iterative procedure is sometimes necessary when significant overlap is encountered. Subsequent subtraction of the ionic resistance and the grain boundary dispersion, followed by a parallel subtraction of the double layer capacitance (CPE) yields finally the charge transfer resistance and the diffusion term (CPE) of the assumed Randles type electrode process, see Fig. 5.

In this process it is important to understand the influence of propagating subtraction errors, which can lead to apparent 'extra dispersion features'. But in the following full CNLS-procedure these errors are generally eliminated (corresponding parameters set to zero or infinite) or the corresponding parameters show very large error estimates. The CNLS-model fit, based on the obtained starting values and assembled equivalent circuit, is also presented in Fig. 3. The insert shows the CNLS-fit residuals, which fall mostly well below the

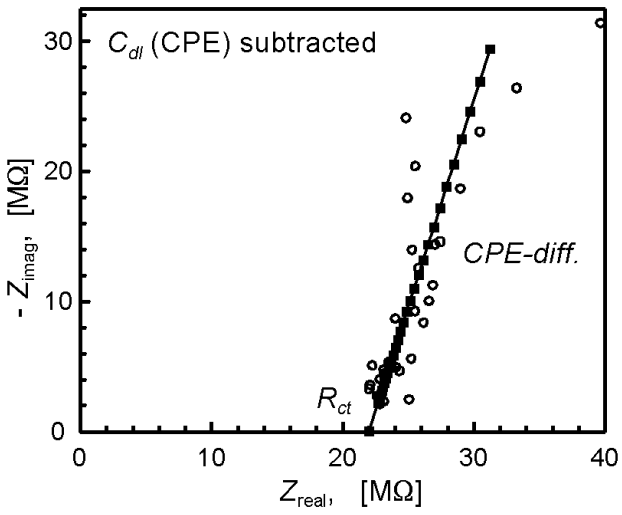

Figure 5: Remaining electrode dispersion after subtraction of the bulk ionic contribution and the double layer capacitance (CPE) from the dispersion of Fig. 4. Solid squares are a fit to the data points.
Bild 5: Verbliebene Elektrodendispersion nach Subtraktion der Beiträge von Ionenleitung und Doppelschichtkapazität (CPE) von der Dispersion in Bild 4. Die schwarzen Quadrate zeigen den Fit zum Datensatz.

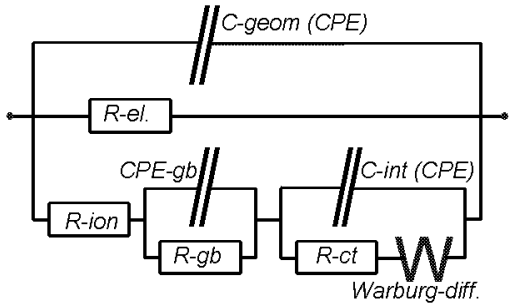

Figure 6: Equivalent circuit that has been assembled during the subtraction procedure. This circuit has been used in the CNLS-fit presented in Fig. 3.
Bild 6: Durch den Subtraktionsprozess entstandenes Ersatzschaltbild, das für den in Bild 3 gezeigten CNLS-Fit verwendet wurde.

0.2% value. This combined analysis procedure leads to the equivalent circuit of Fig. 6, indicating a separate electronic and ionic conduction path. Although ionically blocking gold electrodes have been used, a clear electrode dispersion is observed. This is most likely due to an active oxygen exchange process at the perimeter of the electrode as the sample has both ionic and electronic conductivity [9].

5 Diffusion measurements

Impedance spectroscopy is well suited for the measurement of diffusion processes, e. g. the (de-) intercalation of insertion electrodes like Li_xCoO_2. Although it is also quite easy to do these measurements in the time domain, the analysis may yield incorrect values as no insight is obtained in all other processes (surface transfer, solid electrolyte interface or SEI, etc.) that also influence the current response [10]. In the frequency domain these processes become visible, either from direct inspection of the impedance or through the appropriate de-convolution pre-analysis method. The clear disadvantage is that often very low frequencies are needed to actually uncover the finite length diffusion process. Frequencies below 1 mHz are generally difficult to measure and suffer from noise generated by external signals. It is far easier to measure in the time domain, e. g. by recording the current response to a small voltage step over a period of several hours. The analysis, however, may still be performed in the frequency domain by Fourier transformation of both voltage and current. The impedance is then given by:

$$Z(\omega) = \frac{\overline{V(\omega)}}{\overline{I(\omega)}} \tag{6}$$

where $\overline{V(\omega)}$ and $\overline{I(\omega)}$ represent the Fourier transforms of $V(t)$ and $I(t)$ respectively. The Fourier transform is given by:

$$X(\omega) = \int_0^\infty X(t) \cdot e^{-j\omega t} \mathrm{d}t = \int_0^\infty X(t)\,[\cos \omega t - j \sin \omega t]\,\mathrm{d}t \tag{7}$$

But as we deal with discrete data points, this has to be transformed to a summation. Several methods have been devised to optimize this procedure, but a simple trapezoid summation works well if one is especially interested in the low frequency range of the dispersion [11]:

$$X(\omega) \approx \sum_{k=1}^{N} \frac{X(t_k)\cos \omega t_k - X(t_{k-1})\cos \omega t_{k-1}}{t_k - t_{k-1}} + - j\frac{X(t_k)\sin \omega t_k - X(t_{k-1})\sin \omega t_{k-1}}{t_k - t_{k-1}} \tag{8}$$

An important point of concern is the limited time range of the data. Just ignoring this point can lead to quite some scatter in the transformed set, see the squares in the example of Fig. 7. Extrapolation to infinite time can alleviate this problem. For insertion electrodes the long time behaviour must reach a simple exponential

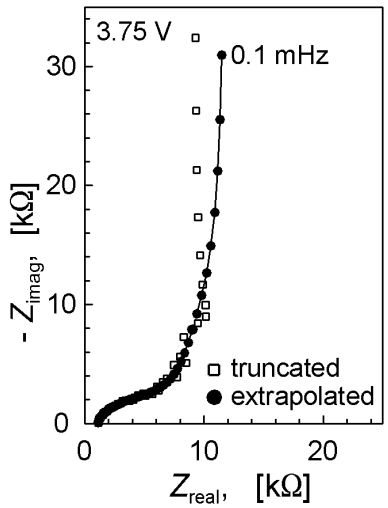

Figure 7: Diffusion impedance of Li-insertion in a Li_xCoO_2 cathode. Transformation from a time-domain measurement with a voltage step of 10 mV [11].
Bild 7: Diffusionsimpedanz für die Li-Insertion in einer Li_xCoO_2-Kathode. Transformation aus der Zeitdomäne mit einer Spannungsstufe von 10 mV [11].

decay. As also a self-discharge or corrosive dc-current may take place, the long-time tail can be modelled by a simple function [11]:

$$X(t) = X_0 + X_1 e^{-t/\tau} \tag{9}$$

which is then used for the extrapolation to infinite time. Here X_0 represents the dc value (self-discharge) that has to be subtracted from the time data. Taking this into account in the complete Fourier transform significantly improves the resulting impedance dispersion as can be seen in Fig. 7 (circles).

This time domain measurement and frequency domain analysis is not restricted to electrochemical systems. For any system, where a time dependent force (potential) and flux (current) can be measured, transformation to the frequency domain will present a much clearer presentation of all processes that are involved in the measured response.

6 Conclusions

Electrochemical Impedance Spectroscopy can be a powerful tool when a number of steps is carefully considered.

- Data validation (Kramers-Kronig transform test) is essential to show to what extent the data is corrupted by non steady state or non-linear behaviour.
- Data deconvolution (successive subtraction procedures) can show small but significant contributions to the overall frequency dispersion.
- Comparison of the residuals of the CNLS model fit to the K-K residuals will indicate the appropriateness of the model.
- Finally, the resulting equivalent circuit should lead to a realistic physical interpretation.

Proper analysis of impedance data from 'complex systems' does require some experience, but the outlined procedures will be helpful in obtaining reliable results.

References

[1] *J.R. Macdonald:* Impedance spectroscopy: old problems and new developments. – In: Electrochim. Acta 35 (1990) Nr. 10, S. 1483–1492.

[2] *B.A. Boukamp:* A non-linear least squares fit procedure for analysis of immittance data of electrochemical systems. – In: Solid State Ionics 20 (1986) Nr. 1, S. 31–44.

[3] *P.R. Bevington*: Data reduction and error analysis for the physical sciences. McGraw-Hill, New York, 1969, chapter 11.

[4] *W.H. Press, B.P. Flannery, S.A. Teukolsky and W.Y. Vettering:* Numerical recipes. Cambridge University Press, Cambridge 1986, S. 289–293.

[5] *J.-L. Dellis and J.-L. Carpentier:* Nelder and Mead algorithm in impedance spectra fitting. – In: Solid State Ionics 62 (1993) Nr. 1–2, S. 119–123.

[6] *M.L. Yang, X.H. Zhang, X.H. Li and X.Z. Wu:* A hybrid genetic algorithm for the fitting of models to electrochemical impedance data. – In: J. Electroanal. Chem. 519 (2002) Nr. 1–2, S. 1–8.

[7] *B.A. Boukamp:* A Linear Kronig-Kramers Transform Test for Immittance Data validation. – In: J. Electrochem. Soc. 142 (1995) Nr. 6, S. 1885–1894.

[8] *B.A. Boukamp:* A package for impedance/admittance analysis. – In: Solid State Ionics 18–19 (1986), S. 136–140.

[9] *B.A. Boukamp, M.T.N. Pham, D.H.A. Blank and H.J.M. Bouwmeester*: Ionic and Electronic Conductivity in Lead-Zirconate-Titanate (PZT). – In: Solid State Ionics 170 (2004) Nr. 3–4, S. 239–254.

[10] *P.J. Bouwman, B.A. Boukamp, H.J.M. Bouwmeester and P.H. Notten:* Influence of Diffusion Plane Orientation on Electrochemical Properties of Thin Film $LiCoO_2$ Electrodes. – In: J. Electrochem. Soc. 149 (2002), Nr. 6 , S. A699–A709.

[11] *B.A. Boukamp:* Electrochemical Impedance Spectroscopy in Solid State Ionics; Recent Advances. – In: Solid State Ionics 169 (2004) Nr. 1–4, S. 65–73.

Dr. Bernard A. Boukamp is assistant professor, connected to the Chair of Inorganic Materials Science at the Faculty of Science and Technology of the University of Twente, The Netherlands.
Major research area: Solid State Electrochemistry and Electrochemical Impedance Spectroscopy.
Address: Fac. of Science and Technology, University of Twente, P.O. Box 217, 7500 AE Enschede, The Netherlands, Tel.: +31.53.4892990, Fax: +31.53.4894683, E-Mail: b.a.boukamp@tnw.utwente.nl